Aqueous extracts of *Moringa oleifera* and *Cinnamomum cassia* as promising sources of antibiofilm compounds against mucoid and small colony variants of *Pseudomonas aeruginosa* and *Staphylococcus aureus*

Eduarda Silva [a] , Pedro Ferreira-Santos [a,c,d], José A. Teixeira [a,b], Maria Olivia Pereira [a,b], Cristina M.R. Rocha [a,b], Ana Margarida Sousa [a,b,*]

[a] Centre of Biological Engineering, LIBRO – Laboratório de Investigação em Biofilmes Rosário Oliveira, University of Minho, Campus de Gualtar, Braga, 4710-057, Portugal
[b] LABBELS – Associate Laboratory, Braga/Guimarães, Portugal
[c] Departamento de Enxeñaría Química, Facultade de Ciencias, University of Vigo, As Lagoas, Ourense 32004, Spain
[d] Instituto de Agroecoloxía e Alimentación (IAA), University of Vigo (Campus Auga), As Lagoas, 32004, Ourense, Spain

ARTICLE INFO

ABSTRACT

Bacterial biofilms formed by *Staphylococcus aureus* and *Pseudomonas aeruginosa* pose significant challenges in treating cystic fibrosis (CF) airway infections due to their resistance to antibiotics. New therapeutic approaches are urgently needed to treat these chronic infections. This study aimed to investigate the antibiofilm potential of various plant extracts, specifically targeting mucoid and small colony variants of *P. aeruginosa* and *S. aureus* and strains. Moreover, it aimed to gain insights into the mechanisms of action and the potential phytochemicals responsible for antibiofilm activity. Solid-liquid extractions were performed on seven biomasses using water and ethanol (70 and 96 %) under controlled conditions, resulting in 21 distinct plant extracts. These extracts were evaluated for extraction yield, antioxidant activity, phenolic content, chemical composition by HPLC-TOF-MS, and antibiofilm activity using a 96-well plate assay, followed by crystal violet staining, bacterial adhesion assessment, and brightfield microscopy. Our findings revealed that aqueous extracts exhibited the highest inhibition of biofilm formation, with cinnamon bark and moringa seeds showing strong antibiofilm activity against both bacterial species. Brightfield microscopy confirmed that these extracts effectively inhibited biofilm formation. Chemical analysis identified key bioactive compounds, including moringin, benzaldehyde, coumarin, and quinic acid, which likely contribute to the observed antibiofilm effects. Recognizing that the antibiofilm properties of moringin, a common compound in both moringa seed and cinnamon bark extracts, remain underexplored, we conducted potential target identification via PharmMapper and molecular docking analyses to provide a foundation for future research. Computational analyses indicated that moringin might inhibit aspartate-semialdehyde dehydrogenase in *P. aeruginosa* and potentially interact with an unknown target in *S. aureus*. In conclusion, moringa seed and cinnamon bark extracts demonstrated significant potential for developing new therapies targeting biofilm-associated infections in CF. Further studies are needed to validate the computational predictions, identify the bacterial targets, and elucidate the precise mechanisms behind moringin's antibiofilm activity, which is likely the potential key contributor to the observed activity of the moringa and cinnamon bark extracts.

1. Introduction

Bacterial infections are a major contributor to the decline in lung function, respiratory failure, and premature death of cystic fibrosis (CF) patients. CF is a genetic disorder characterized by severe airway complications, leading to the accumulation of thick and viscous mucus, which creates a propitious environment for the development of respiratory chronic infections [1,2]. *Staphylococcus aureus* is one of the first pathogens to colonize the airways of CF patients, with a prevalence reaching approximately 75 % in children aged 6–17 years [3]. Meanwhile, *Pseudomonas aeruginosa* is currently considered the most relevant

---

Abbreviations

ASADH	aspartate-semialdehyde dehydrogenase
CF	Cystic fibrosis
CFU	colony forming unit
CV	crystal violet
DMSO	Dimethyl sulfoxide
DPPH	2,2-diphenyl-1-picrylhydrazyl
EPS	Extracellular polymeric substance
FRAP	Ferric Reducing Antioxidant Power
MRSA	methicillin-resistant *Staphylococcus aureus*
QS	quorum sensing
RMSD	root-mean-square deviation
SEB	*Staphylococcus aureus* enterotoxin B
SCV	Small colony variant

pathogenic agent responsible for chronic infection development, decreased quality of life, long hospitalizations, and ultimately the high number of deaths [4–6].

Biofilm formation plays a central role in the long-term persistence and resistance of both *S. aureus* and *P. aeruginosa*. Biofilms provide multifactorial mechanisms that contribute to antibiotic resistance, including restricted penetration of antibiotics through the matrix, slow growth of bacteria due to nutritional constraints and restricted oxygen penetration, quorum sensing (QS), expression of biofilm-specific genes, and the presence of persister cells [2,6,7]. Additionally, biofilms facilitate interactions between bacterial species in CF lungs, which can enhance resistance to antibiotics through coordinated activities [8,9]. Depending on the age, 40–95 % of CF patients are coinfected with *P. aeruginosa* and *S. aureus* [3], and these coinfections often result in more severe effects on lung function and poorer clinical prognosis compared to mono-infections, which explain the biofilm relevance in CF disease [10].

A particularly challenging aspect of CF-related infections is the presence of small colony variants (SCV) and the mucoid phenotype. SCV of *S. aureus* and *P. aeruginosa* are slow-growing populations that exhibit increased resistance to antibiotics and immune response due to their altered metabolism, ability to survive under the nutrient-depleted and anaerobic conditions of CF lungs, and intracellular survival [11–14]. These adaptations allow SCV to evade conventional therapies, contributing to chronic infection and the progressive decline in lung function [12,14]. Similarly, the mucoid phenotype of *P. aeruginosa*, which is characterized by excessive alginate production, an exopolysaccharide that creates a protective barrier around the bacteria, is strongly linked to chronic infections and antibiotic resistance. This alginate matrix enhances biofilm formation, complicating treatment and resulting in more severe lung damage [15–17].

Over the past decades, therapeutic advancements, such as Cystic Fibrosis Transmembrane Conductance Regulator (CFTR) modulators that target the CFTR protein responsible for regulating chloride and sodium ion transport across cell membranes, and mucoactive drugs have significantly increased the survival of CF patients, with a median age at death rising to 36.9 years in 2023 [18–21]. Although these drugs have notably improved disease management [19,20], they have no reported effect on bacterial infections. Antibiotics remain the cornerstone of CF treatment, however, they are not specifically designed to target biofilms, underscoring the pressing need for compounds in CF therapeutic regimes that can alter the physiological state of antibiotic-tolerant biofilm cells to enhance antibiotic efficacy [22].

Plants have shown great potential as therapeutic agents, offering anti-inflammatory, anticancer, antioxidant, and antimicrobial properties. They have been a valuable source in providing chemical architectures for the drug discovery pipeline of antibiofilm drugs [23–25]. For instance, *Camellia sinensis* (L.) Kuntze (tea plant) was shown to reduce *P. aeruginosa* biofilm biomass and weaken biofilm structure, while also reducing the expression of several virulence factors [26]. Also, the seeds of *Capsicum baccatum* var. *pendulum* (Willd.) Eshbaugh (red pepper) interfered with *P. aeruginosa* bacterial adhesion to the surface and only allowed the formation of smaller cell clusters without biofilm matrix [27]. Regarding *S. aureus*, both *Melaleuca alternifolia* (Maiden & Betche) Cheel (tea tree) and leaves of *Duabanga grandiflora* (Roxb. Ex DC.) Walp. (Lamphu Tree) reduced the bacterial attachment to the surface, leading to the formation of weak biofilms, with tea tree being able to target methicillin-resistant *Staphylococcus aureus* (MRSA) [28,29]. A water extract of *Artemisia princeps* Pamp. (mugwort) also showed activity against MRSA inhibiting biofilm formation and the expression of some virulence genes, including *mecA*, *sea*, *agrA*, and *sarA* involved in the biofilm formation [30].

Plant extracts are complex mixtures of a variety of compounds, such as proteins, carbohydrates, lipids, and secondary metabolites. The antibiofilm activity of several plant extracts is often attributed to their secondary metabolites, or phytochemicals, including phenolics. Plant extracts rich in phenolic compounds have shown the ability to inhibit biofilms by different mechanisms; including reducing bacterial virulence [31], interfering with quorum-sensing [32] or disrupting mature biofilms [33].

Despite extensive research into antibiofilm drug discovery, no effective treatment specifically targeting biofilms in CF lungs currently exists, and antibiofilm agents are not yet part of standard CF therapeutic regimes. Developing plant-based antibiofilm drugs to prevent biofilm formation remains a significant challenge, representing a novel and promising avenue in drug discovery and development. To the best of our knowledge, this study is the first to investigate the antibiofilm activity of plant extracts specifically against mucoid and SCV strains of *P. aeruginosa,* and *S. aureus*. The objective of this study is to identify potent candidate extracts, elucidate their mechanism of action and identify phytochemicals responsible for antibiofilm activity, with the potential to progress these findings into drug discovery and development for CF treatment. The selected plants, eucalyptus (*Eucalyptus globulus* Labill.), broom flowers (*Cytisus scoparius* (L.) Link), pine (*Pinus pinaster* Aiton), moringa (*Moringa oleifera* Lam.), cinnamon (*Cinnamomum cassia* (L.) J.Presl) and lemongrass (*Cymbopogon citratus* (DC.) Stapf), were chosen based on their documented antimicrobial and antioxidant properties, as well as their known antibiofilm activity against bacteria [25,34–36].

2. Materials and methods

2.1. Plant material

Eucalyptus leaves (*Eucalyptus globulus* Labill.) and broom flowers (*Cytisus scoparius* (L.) Link) were collected in Braga, Portugal, in September 2021 and in April 2022, respectively. Pine bark (*Pinus pinaster* Aiton) was collected in Ponte de Lima, Portugal, in April 2019. Moringa seeds and leaves (*Moringa oleifera* Lam.) were collected in Ceará, Brazil, in December 2017. Cinnamon bark (*Cinnamomum cassia* (L.) J.Presl) and lemongrass (*Cymbopogon citratus* (DC.) Stapf) were purchased from a local supermarket. The plant parts were washed, dried and milled to a fine powder.

2.2. Extractions

Solid-liquid extractions were performed in a water bath at 70 °C and 150 rpm for 1 h, using different solvents aiming at obtaining extracts rich in compounds with different polarities: water, ethanol 70 % (v/v) (EtOH70) or ethanol 96 % (v/v) (EtOH96), in triplicate. The extractions used a solid load of 5 % (2 g of dry plant biomass in 40 mL of solvent). After the extraction process, the product was filtered under vacuum. Liquid extracts were then analysed to determine the extraction yield and

the extract concentration, antioxidant activity, and total phenolic content. The remaining extracts were stored at −20 °C until further chemical characterization and microbiology assays.

2.3. Extraction yield

The concentration of each extract was determined gravimetrically. Specifically, 1 mL of extract was dried overnight at 105 °C and the weight of the dry extract was measured. The test was made in triplicate. The extraction yield (expressed in %) was calculated as shown in Equation (1):

$$\text{Extraction yield (\%)} = \frac{\text{dried extract (g)}}{\text{initial liquid extract (g)}} \times 100 \quad (1)$$

2.4. Antioxidant activity

2.4.1. Ferric Reducing Antioxidant Power
Antioxidant activity was determined using the Ferric Reducing Antioxidant Power (FRAP) assay [37]. 6-Hidroxy-2,5,7,8-tetra-methyl-chromone-2-carboxylic acid (Trolox), prepared in methanol, was used as standard. The 2,4,6-Tripyridyl-*s*-Triazine solution (TPTZ) with 10 mM was prepared in 40 mM HCl and the ferric chloride solution at 20 mM was prepared in water. The FRAP working solution was prepared by mixing 10-vol of acetate buffer at 300 mM (pH 3.6) with 1-vol of TPTZ and 1-vol of ferric chloride. The mixture was composed of 20 µL of liquid extracts resulting from each extraction and 280 µL FRAP working solution. The mixture was incubated at 37 °C for 30 min, protected from light, and the absorbance was measured at 595 nm. Antioxidant activity was expressed as milligrams of Trolox equivalent *per* milligram of dry extract (mg TEAC/mg extract). Analyses were performed in triplicate.

2.4.2. 2,2-Diphenyl-1-picrylhydrazyl (DPPH) scavenging activity
Antioxidant activity was also determined by the 2,2-diphenyl-1-pic-rylhydrazyl (DPPH) radical scavenging assay [38]. Trolox, prepared in methanol, was used as standard. The mixture was composed of 20 µL of liquid extracts resulting from each extraction and 180 µL DPPH solution (150 µM, dissolved in 80 % methanol). The mixture was incubated at room temperature for 30 min, protected from light, and the absorbance was measured at 515 nm. DPPH radical scavenger activity was calculated as shown in Equation (2):

$$\% \text{ inhibition} = \frac{\text{Ac} - \text{As}}{\text{Ac}} \times 100 \quad (2)$$

where Ac is absorbance of control and As is absorbance of sample. Results were expressed as milligrams of Trolox equivalent *per* milligram of dry extract (mg TEAC/mg extract). Analyses were performed in triplicate.

2.5. Total phenolic content

Total phenolic content was determined according to the Folin-Ciocalteu method [39]. The reaction mixture was composed of 20 µL of liquid extract resulting from each extraction, 100 µL Folin-Ciocalteu reagent 10 % (1:10 in water) and 80 µL of sodium carbonate 75 g/L. The mixture was incubated at 42 °C for 30 min, protected from light. The absorbance was measured at 750 nm using a microplate reader. Gallic acid was used as standard. Total phenolic content was expressed as milligrams of gallic acid equivalents *per* milligrams of extract (mg GAE/mg extract), and phenolic extraction yield was expressed as milligrams of gallic acid equivalents *per* gram of dry matrix (mg GAE/g matrix). Analyses were performed in triplicate.

2.6. HPLC-TOF-MS

An exploratory identification of phytochemicals compounds recovered was performed using high-performance liquid chromatography (HPLC) time-of-flight mass spectrometry (HPLC-TOF-MS). The plant extracts were injected into a ZORBAX Eclipse XDB-C18 fast resolution HD (2.1 × 100 mm 1.8 µm de Agilent), and the HPLC separation was performed using an Elute HPLC from Bruker Daltonics. The mobile phases used were 0.1 % formic acid in water (solvent A) and acidified acetonitrile with 0.1 % formic acid (solvent B), with a flow rate of 0.4 mL/min. The linear gradient was as follows: 2 % solvent B over 2 min, 2 %–30 % solvent B over 13 min, 30 %–100 % solvent B over 2 min, 100 % solvent B over 4 min, 100 %–2 % solvent B over 1 min, and 2 % solvent B isocratically for 2 min. An ESI source created ions in negative and positive ion mode. The operating circumstances were as follows: 3000 V capillary voltage, 500 V end plate offset, 8.0 L/min dry gas, 2 bar nebulizer pressure, and a dry heater set to 220 °C. Metabolite identification was based on reliable mass data, isotopic pattern matching (mSigma value), retention duration (where a standard was provided), and substances reported in literature.

2.7. Bacterial strains and culture conditions

The antibiofilm activity of the extracts was determined using two strains of *S. aureus* including ATCC 25923 and a CF clinical isolate with SCV phenotype, named SA-1 and SA-SCV, respectively. Additionally, three *P. aeruginosa* strains were included: two CF clinical isolates, representing a mucoid phenotype and a SCV phenotype, named PA-Muc and PA-SCV respectively, and a non-CF isolate named PAI. The clinical isolates used in this study were generously provided by various Portuguese Hospitals. These strains were selected based on their phenotypic characteristics to represent the variety of strains commonly isolated from CF patients. Bacteria were routinely cultured on Tryptic Soy Broth (TSB, Liofilchem) or Tryptic Soy Agar (TSA, Liofilchem) at 37 °C. All strains were preserved in cryovials (Nalgene) at −80 ± 2 °C. Prior to each experiment, bacterial cells were grown on TSA plates overnight at 37 °C.

2.8. Biofilm formation inhibition assay

Serial concentrations of plant extracts were tested in 96-well microtiter plates with flat bottoms (Orange) using TSB, with 100 µL of extracts in each well. For the ethanolic and hydroethanolic extracts, before the serial dilutions, the solvent was first evaporated using nitrogen and then the extract was dissolved in 5 % of dimethyl sulfoxide (DMSO). Overnight inocula of each bacteria strain were washed twice in sterile water by centrifugation (9000 *g*, 5 min) and further serial diluted in sterile water. The cell suspensions were added to 96-well microtiter plates (100 µL *per* well) to obtain a final concentration of 1×10^7 CFU/mL. The plate was then incubated for 24 h at 37 °C and 120 rpm to allow biofilm formation. After 24 h of growth, planktonic cells (liquid content of the wells) were removed, and each well was washed twice with distilled water. Biofilm formation was determined using the crystal violet (CV) method [40]. 200 µL of methanol was added to each well to fix the biofilm for 15 min. After the wells dried out, CV (1 %) was added to dye biofilms for 5 min and washed twice with distilled water. 200 µL of glacial acetic acid (33 %) was added and mixed (pipette up and down) with CV retained by biofilm biomass. The absorbance was measured at 570 nm using a microplate reader. Biofilm inhibition was calculated as shown in Equation (3)

$$\% \text{ inhibition} = \frac{\text{Au} - \text{Ae}}{\text{Au}} \times 100 \quad (3)$$

where Au is the absorbance of untreated biofilm and Ae is the absorbance of biofilm treated with extract. Analyses were performed, at least three times and the results are expressed in percentage of biofilm inhibition.

2.9. Assessment of bacterial adhesion

The viability of *P. aeruginosa* and *S. aureus* cells adhered after the application of plant extracts was determined through colony-forming unit (CFU). The formation of biofilm was performed in 96-well plates flat bottom (Orange) as described in section 2.8. After 24 h of growth, planktonic cells were removed, and each well was washed twice with distilled water. 200 μL of distilled water was added to each well and the plate placed on an ultrasonic water bath for 10 min to release the biofilm cells from the well surface as previously optimized [41]. The content of five wells was transferred to a microcentrifuge tube to make up a volume of 1 mL and vortexed to homogenise the cell suspensions. Afterwards, the cell suspensions were serially diluted and plated on TSA to determine the number of culturable cells adhered to the wells. After overnight growth at 37 °C, CFUs were counted. Analyses were performed in triplicate and the results were expressed as $\log_{10}$ CFU *per* volume (mL).

2.10. Assessment of antibiofilm activity by brightfield microscopy

Brightfield microscopic assessment of all bacterial biofilms was accomplished to investigate the antibiofilm activity. The methodology described in section 2.8 was slightly altered to allow the biofilm formation on a coverslip. Briefly, a plastic coverslip (Thermanox) was placed on the bottom of wells in a 24-well plate and 1 mL of the selected concentration of each extract was added to the well on top of the coverslip. Further, 1 mL of bacterial suspension from overnight inocula was added to the wells to make a total volume of 2 mL and a final concentration of 1×10^7 CFU/mL. The plate was incubated for 24 h at 37 °C and 120 rpm to allow biofilm formation. After 24 h growth, the well liquid content was removed, leaving the coverslip in place, and each well was washed twice with distilled water. The coverslip was stained using the CV method as described previously with slight alterations. 500 μL of methanol was added to each well to fix the biofilm to the coverslip and after 15 min, methanol was removed. After the coverslips dried out, 500 μL of CV reagent (1 %) was added to dye the biofilm for 5 min. The excess stain was washed off using distilled water, and the coverslip was placed on a microscope glass slide to observe the biofilms under a brightfield microscope (10× magnification) (Olympus BX51TF).

2.11. Targets prediction

Putative targets of the most abundant phytochemical, moringin, were predicted using PharmMapper [42]. The parameters set in PharmMapper included a Maximum of 300 Generated Conformations and selecting 'all targets' option [43,44]. The results were ranked by normalized fit-score.

2.12. Molecular docking

RCSB-Protein Data Bank [45] was used to obtain the three-dimensional (3D) structure of proteins from *P. aeruginosa* and *S. aureus* indicated by PharmMapper. The 3D structure of the moringin was obtained from PubChem (ID 153557) [46] in.sdf format. The protein structure was pre-processed using the protein preparation wizard, which involved adding the missing residues in the crystal structure and removing the water molecules surrounding the receptor. Moringin was individually docked with the two proteins using the molecular docking software AutoDock 4.2.6 [47]. The docking procedure followed previously established protocols, with a grid size configured for blind docking. The grid box was set to 126 x 126 x 126 for x, y and z axis, respectively, using Autogrid program in such a way that encompass the entire molecule of moringin. Docking simulation were carried out using the Lamarckian genetic algorithm with default parameters. The docking protocol included 100 different runs (RMSD tolerance of 2.0 Å) with a population size of 150 and a maximum number of evaluations of 25 000

000 (set to 'long'). After each docking calculation, the generated docked conformations were ranked based on predicted binding energy. The best energy conformation of the moringin (ligand)-protein complex and orientation of the ligand at the binding site were analysed using USCF Chimera 1.8 (RBVI, USA) and Biovia Discovery Studio [48].

2.13. Statistical analysis

All data was analysed using GraphPad Prism software package (GraphPad Software version 8). Statistical analysis was carried out by ANOVA with Tukey's multiple comparison. Differences were considered statistically significant at $p < 0.05$.

3. Results

3.1. Extraction yield, antioxidant activity and phenolic content

This study was designed to obtain a diverse range of extracts from six plants, using solvents with varying polarities (water > EtOH70 > EtOH96) to maximize the potential for identifying a potent antibiofilm plant extract. Extracts with higher phenolic content often exhibit greater antioxidant activity, which can correlate with enhanced antibiofilm effects. Before evaluating antibiofilm activity, the effects of the extraction procedures on extraction yield, antioxidant activity, and phenolic content were analysed (Table 1).

Eucalyptus leaf extracts showed the highest phenolic yields when extracted with water and EtOH70, but lower yields with EtOH96. Despite the lower total phenolic content of the EtOH96 extract, its antioxidant activity was highest along with water and EtOH70 extracts.

Moringa seed extracts showed extremely low phenolic extraction yield and content, along with no notable antioxidant activity. Likewise, moringa leaf extracts showed low phenolic content and antioxidant activity, despite having moderate phenolic yield when extracted with water.

Cinnamon bark extracts showed the lowest values across all parameters when using EtOH96 and showed moderate values of antioxidant activity with the other two solvents. Pine bark extracts displayed higher values across all parameters tested when extracted with EtOH70. Both broom flower and lemongrass extracts showed low phenolic yield and content and antioxidant activity across all solvents, with EtOH70 performing slightly better in extracting phenolic compounds and antioxidant activity, and overall extraction yield. For lemongrass, though the extraction yield was higher when using water or EtOH70, the highest phenolic content was obtained when using EtOH96.

Overall, our results indicated that a high phenolic content generally corresponds to a high antioxidant activity across all biomasses. However, some exceptions were observed, suggesting that other components in the extracts may be responsible for the antioxidant activity. Additionally, there was no specific correlation between the antioxidant activity and the solvent polarity, as it depended on the biomass being extracted.

3.2. Assessment of antibiofilm activity and chemical composition of the extracts

The antibiofilm effect of the plant extracts was determined, revealing significant variations among the extracts and also between the solvents used for extraction. Antibiofilm activity was considered promising if an extract inhibited, at least, 75 % of biofilm formation.

Aqueous extracts (Fig. 1) showed superior inhibition rates of biofilm formation for all biomasses tested compared to the ethanolic extracts (Supplemental material, Figs. S1 and S2). With a few exceptions, aqueous extracts showed a dose-dependent inhibitory effect on the biofilm formation, achieving higher inhibition rates at the highest concentrations. The antibiofilm effect also depended on the strain tested for both species.

Table 1

Characterization of plant extracts: extraction yield, phenolic yield, phenolic content, FRAP, and DPPH. Values represent mean ± standard deviation of three independent experiments. Statistical analysis was performed for the three extracts for each biomass. Identical letters within the same biomass indicate no statistically significant differences between extracts. Different letters indicate statistically significant differences ($p < 0.05$).

Plant Solvent	Extraction yield (%)	Phenolic yield (mg GAE/g matrix)	Total Phenolic Content (mg GAE/mg extract)	FRAP (mg TEAC/mg extract)	DPPH (mg TEAC/mg extract)
Eucalyptus leaves					
Water	15.80 ± 0.40[a]	56.16 ± 9.15[a]	0.36 ± 0.06[a]	0.41 ± 0.01[a]	0.78 ± 0.02[a]
EtOH70	22.40 ± 1.60[b]	60.29 ± 0.67[a]	0.27 ± 0.01[b]	0.16 ± 0.02[b]	0.58 ± 0.03[b]
EtOH96	9.00 ± 0.40[c]	8.31 ± 0.57[b]	0.09 ± 0.01[c]	0.31 ± 0.03[c]	0.78 ± 0.01[a]
Moringa seeds					
Water	13.10 ± 0.70[a]	1.95 ± 0.16[a]	0.02 ± 0.001[a]	0.01 ± 0.001[a]	0.01 ± 0.001[a]
EtOH70	9.00 ± 1.00[b]	2.03 ± 0.09[a]	0.02 ± 0.001[a]	0.01 ± 0.001[a]	0.01 ± 0.002[a]
EtOH96	7.50 ± 0.10[b]	2.43 ± 0.22[a]	0.03 ± 0.003[a]	0.01 ± 0.001[a]	0.02 ± 0.003[a]
Moringa leaves					
Water	39.67 ± 7.84[a]	31.15 ± 0.75[a]	0.08 ± 0.007[a]	0.12 ± 0.00[a]	0.07 ± 0.004[a]
EtOH70	25.00 ± 1.00[b]	13.90 ± 0.80[b]	0.06 ± 0.004[a]	0.10 ± 0.01[ab]	0.05 ± 0.004[a]
EtOH96	11.60 ± 1.00[c]	6.48 ± 0.18[c]	0.05 ± 0.001[a]	0.08 ± 0.01[b]	0.04 ± 0.006[a]
Cinnamon bark					
Water	6.30 ± 2.70[a]	11.69 ± 0.36[a]	0.19 ± 0.01[a]	0.33 ± 0.03[a]	0.32 ± 0.05[a]
EtOH70	14.60 ± 1.41[b]	25.30 ± 0.77[b]	0.17 ± 0.01[a]	0.15 ± 0.01[b]	0.53 ± 0.001[b]
EtOH96	7.00 ± 1.50[a]	3.91 ± 0.18[c]	0.06 ± 0.003[b]	0.02 ± 0.002[c]	0.19 ± 0.03[c]
Pine bark					
Water	4.83 ± 1.19[a]	10.37 ± 0.34[a]	0.21 ± 0.007[a]	0.54 ± 0.00[a]	0.48 ± 0.02[a]
EtOH70	10.4 ± 0.60[b]	28.90 ± 0.51[b]	0.29 ± 0.01[b]	0.75 ± 0.02[b]	0.63 ± 0.21[b]
EtOH96	11.8 ± 1.20[b]	19.31 ± 0.36[c]	0.18 ± 0.003[a]	0.51 ± 0.01[c]	0.38 ± 0.04[c]
Broom flowers					
Water	18.80 ± 1.20[a]	5.63 ± 0.08[a]	0.03 ± 0.001[a]	0.05 ± 0.001[a]	0.03 ± 0.003[a]
EtOH70	25.6 ± 1.40[b]	16.35 ± 0.32[b]	0.06 ± 0.002[b]	0.13 ± 0.01[b]	0.07 ± 0.05[b]
EtOH96	14.70 ± 0.30[a]	6.34 ± 0.04[a]	0.04 ± 0.001[ab]	0.11 ± 0.005[b]	0.05 ± 0.004[ab]
Lemongrass					
Water	18.30 ± 2.12[a]	6.06 ± 0.20[a]	0.03 ± 0.001[a]	0.08 ± 0.002[a]	0.05 ± 0.002[ab]
EtOH70	17.15 ± 0.35[a]	7.75 ± 1.08[ab]	0.05 ± 0.002[a]	0.14 ± 0.004[b]	0.07 ± 0.05[a]
EtOH96	7.50 ± 0.10[b]	10.93 ± 2.27[b]	0.14 ± 0.03[b]	0.08 ± 0.007[a]	0.03 ± 0.004[b]

DPPH: 2,2-diphenyl-1-picrylhydrazyl; FRAP: Ferric Reducing Antioxidant Power; GAE: gallic acid equivalent; TEA: Trolox equivalent.

The extracts from eucalyptus showed the strongest reduction of biofilm formation of *S. aureus* with approximately 100 % inhibition rate at a concentration of 3.9 mg/L (Fig. 1A). The extracts from moringa seeds and cinnamon showed the strongest reduction of biofilm formation in both *P. aeruginosa* and *S. aureus* at 3.3 and 1.6 mg/mL, respectively (Fig. 1B and D). Weak biofilm inhibition was observed for the extracts of moringa leaves, pine bark, broom flower and lemongrass (Fig. 1C–E, F and G).

In an attempt to identify the compounds responsible for the antibiofilm activity in aqueous extracts, a HPLC-TOF-MS analysis focused on phenolic compounds was conducted. Detailed mass spectra data, absorbance spectra, and retention times were compared with the available literature. The names, molecular weight, molecular formula, mass-to-charge ratio and mSigma of each component in the extracts are presented in Table 2.

The moringa seed and leaf extracts were rich in moringin and benzaldehyde, with adenosine, hydrocinnamic acid and citric acid also in abundance in the extracts. In the extracts from cinnamon bark, coumarin, quinic acid, and moringin were the most abundant compounds. A strong presence of moringin was also found in lemongrass extract, but kaempherol was the most abundant. The broom flower extract was constituted mostly by chrysin, anhydroglycinol and kaempherol, while the eucalyptus extract contained several abundant compounds, including quinic acid, citric acid, 3,4-dihydroxybenzoic acid, azelaic acid, kaempherol and pyrogallol. Notably, 6-gingerol was found in all extracts analysed.

3.3. Effect on bacterial adhesion and biofilm formation

Based on significant antibiofilm activity against both species, aqueous extracts of moringa seeds and cinnamon were selected for further investigation to elucidate their potential mechanism of action. Their activity against both species is particularly pertinent for CF management disease and the reason for their drug discovery studies.

Quantitative assessment of bacterial adhesion to the surface was initially performed by CFU counting. Obtained results revealed that the surfaces were populated by an increased number of bacterial cells, with no differences observed in *P. aeruginosa* with respect to the control group (untreated biofilms) (Fig. 2). However, extracts from moringa seeds and cinnamon bark reduced the adhered bacterial load of *S. aureus* by 3 log.

In situ visualization of surfaces by brightfield microscopy confirmed an increased number of bacteria adhered to surfaces and the absence of biofilm formation or aggregates. Bacterial cells treated with extracts of moringa seeds (Fig. 3F, G, H, I, J) and cinnamon bark (K, L, M, N, O) were scattered across the surface, in opposite to the densely packed biofilm structures observed in the control group (Fig. 3A–E). It should be noted that both extracts, especially moringa, left residues after 24 h that deposited on surfaces and were stained by CV (indicated by red arrows in Fig. 3), which may be mistaken for biofilms or cell aggregates in brightfield microscopy images (Supplemental material, Fig. S3).

3.4. Target prediction and molecular docking

The compound moringin, abundant in both moringa seed and cinnamon extracts, is likely a key contributor to the antibiofilm properties of these extracts. Given the limited research on the antibiofilm properties of moringin and to lay the groundwork for future research in this compound, we sought to identify its potential targets in *P. aeruginosa* and *S. aureus* and perform molecular docking to assess the plausibility of the proposed targets and their interaction with moringin.

To explore its potential molecular targets, the PharmMapper web server was used for reverse pharmacophore mapping. PharmMapper compared the pharmacophores of the moringin against an in-built database of pharmacophore models, providing target information for 300 proteins along with their fit-score and number of pharmacophoric features. Target selection by PharmMapper was further refined using protein data retrieved from the RCSB-Protein Data Bank [45] with a focus on the proteins relevant to *P. aeruginosa* and *S. aureus*. Table 3
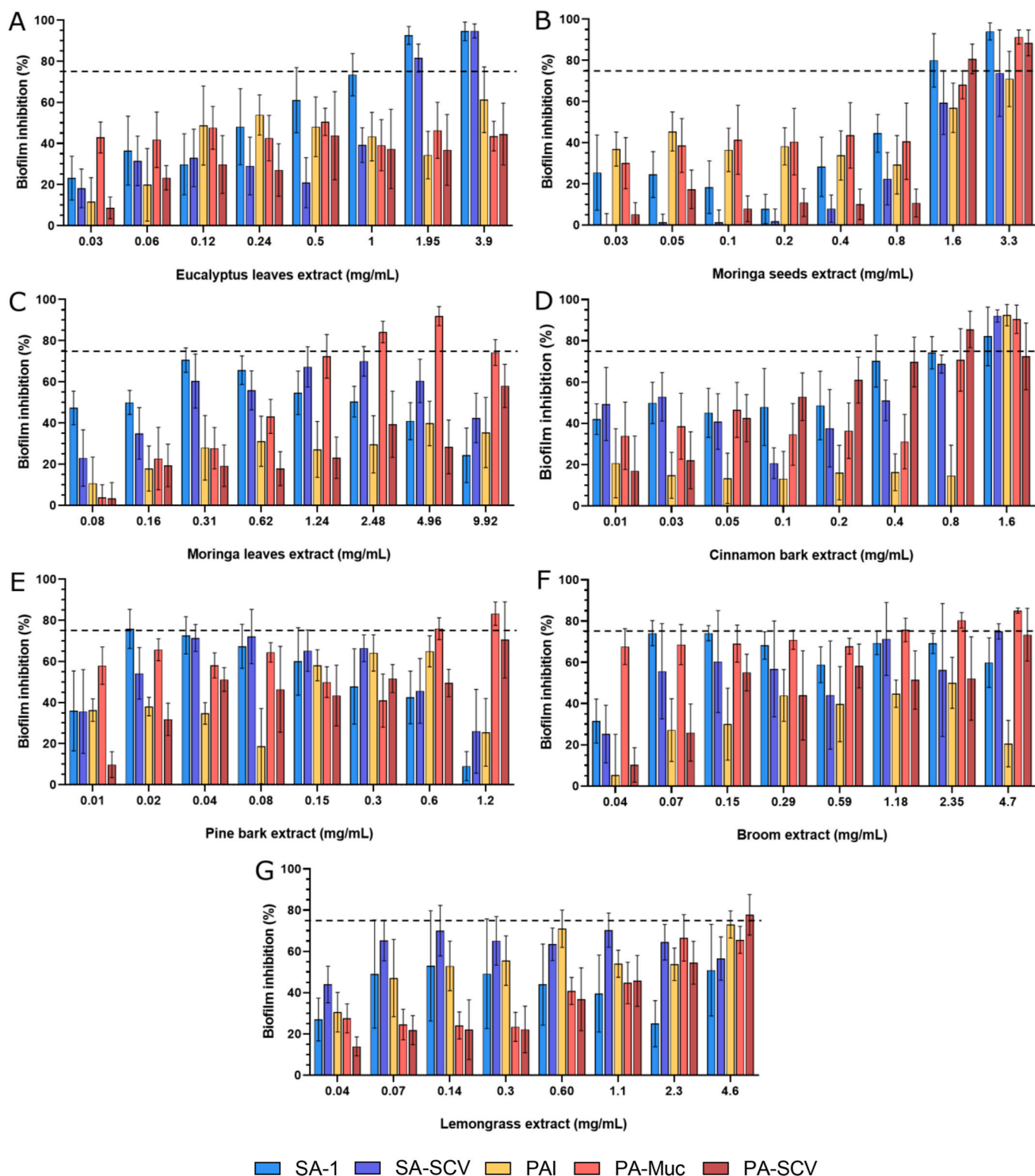
Fig. 1. Inhibition of biofilm formation by the aqueous extracts of **(A)** Eucalyptus leaves, **(B)** Moringa seeds, **(C)** Moringa leaves, **(D)** Cinnamon bark, **(E)** Pine Bark, **(F)** Broom flowers, **(G)** Lemongrass. Values represent mean ± standard deviation of, at least, 3 independent experiments. Inhibition of biofilm formation expressed in percentage (%) and extracts concentration in mg/mL. Dashed line represents the minimum value for promising antibiofilm activity (75 % of inhibition rate).

shows the potential targets for moringin after filtering for proteins associated with these bacterial species. Aspartate-semialdehyde dehydrogenase (ASADH, PDB ID: 2HJS) was identified as a potential target for *P. aeruginosa,* while the HLA-DR4 complexed with peptide and SEB (*Staphylococcus aureus* enterotoxin B) (PDB ID: 1D5M) was associated to *S. aureus*. HLA-DR4 is a human MHC class II receptor that binds bacterial

enterotoxins to mediate immune responses [49,50]. However, as our experiments were conducted *in vitro* using bacterial biofilms without a host immune component, the relevance of this complex in our study was not supported. Consequently, further computational investigations involving HLA-DR4 are presented in the supplemental material.

Molecular docking simulations were conducted to predict the

Table 2

Extracts' composition identified by HPLC-TOF-MS. Values presented as signal intensity: , absent; +, present (<50000); ++, abundant (50000–1000000); +++, highly abundant (>1000000).

RT [min]	m/z measure	mSigma	Compound	Molecular Formula	Mw	EL	MS	ML	CB	PB	LG	BF
0.73	191.05577	2.1	Quinic acid	C7H12O6	192.06	++	–	++	+++	++	++	+
0.78	191.01942	2.5	Citric acid	C6H8O7	192.03	++	++	++	++	++	+	++
0.82	153.01873	6.3	3,4-Dihydroxybenzoic acid	C7H6O4	154.03	++	–	–	+	++	+	+
0.83	137.02389	12.4	2,5-Dihydroxybenzaldehyde	C7H6O3	138.03	+	+	+	++	++	++	++
0.83	125.02411	4.6	Pyrogallol	C6H6O3	126.03	++	+	–	+	++	+	+
0.84	109.0294	3.6	1,2-Benzenediol	C6H6O2	110.04	+	+	–	+	+	+	+
0.94	187.09729	10.6	Azelaic acid	C9H16O4	188.10	++	++	+	+	+	++	++
20.2	285.0413	13.6	Kaempferol	C15H10O6	286.05	++	–	+	–	+	+++	+++
21.53	356.08044	4.6	Moringin	C14H17NO5S	311.08	+	+++	+++	+++	–	++	+
22.81	193.08657	16.7	Deoxyarbutin	C11H14O3	194.09	+	+	+	+	+	+	+
23.06	253.05036	12.8	Anhydroglycinol	C15H10O4	254.06	–	++	+	+	++	–	+++
23.67	293.17572	5.2	6-Gingerol	C17H26O4	294.18	++	++	++	++	++	++	++
24.3	375.13955	17	Erianin	C18H22O5	318.15	+	+	+	+	+	+	+
0.77	268.10381	19.6	Adenosine	C10H13N5O4	267.10	–	++	++	+	+	++	–
0.81	133.06371	3.8	Hydrocinnamic acid	C9H10O2	150.07	+	++	++	++	+	+	+
13.93	147.04363	5.6	Coumarin	C9H6O2	146.04	+	++	–	+++	+	+	+
15.32	303.04927	5.8	Quercetin	C15H10O7	302.04	+	–	++	–	–	–	+
21.53	107.04889	5.6	Benzaldehyde	C7H6O	106.04	+	+++	+++	++	+	++	–
21.79	271.05926	10.2	Galangin	C15H10O5	270.05	+	+	–	–	+	+	++
21.96	301.07021	16.7	Kaempferide	C16H12O6	300.06	+	–	+	–	+	+	++
22.67	233.15271	11	Isoalantolactone	C15H20O2	232.15	++	–	+	+	+	+	+
22.86	203.1791	42.3	alpha-curcumene	C15H22	202.17	++	+	–	+	++	–	++
23.01	279.23147	15.4	a-Linoleic acid (NMR)	C18H30O2	278.22	+	+	+	+	++	+	+
23.06	255.06464	7.6	Chrysin	C15H10O4	254.06	–	+	–	+	+	–	+++

BF: Broom flowers; CB: Cinnamon bark; EL: Eucalyptus leaves; LG: Lemongrass; ML: Moringa leaves; MS: Moringa seeds; PB: Pine bark.
Mw: molecular weight, m/z: mass to charge ratio, RT: retention time.
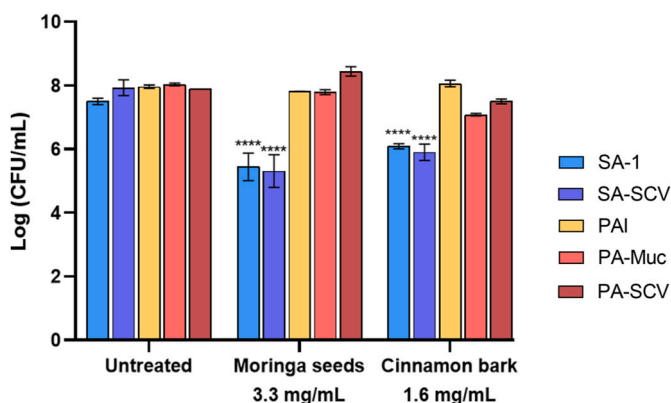

Fig. 2. Adhesion of bacterial cells to the surface after treatment with aqueous extracts of moringa seeds (3.3 mg/mL) and cinnamon bark (1.6 mg/mL). Values represent mean ± standard deviation of 3 independent experiments. The differences in $\log_{10}$ CFU/mL of the bacterial growth after the application of the extracts were compared to the untreated populations using two-way ANOVA followed by Tukey's multiple comparison. Significant differences are indicated by asterisks: $*p < 0.05$, $**p < 0.01$, $***p < 0.001$, $****p < 0.0001$.

binding modes and affinities of moringin with ASADH and HLA-DR4 complexed with peptide and SEB, separately. Moringin demonstrated varying degrees of interaction with the target proteins (Supplemental material, Fig. S4). Cluster analysis indicated that optimal binding conformations were obtained in the 33rd and 55th runs, which correspond to the lowest binding energy (Table 4), with 2 and 4 conformations identified for moringin-ASADH and moringin-HLA-DR4 complexes, respectively.

The estimated inhibition constant (Ki) provided further insights into the compounds' inhibitory potency, with lower Ki values indicating stronger inhibitory potential. Moringin exhibited significantly low Ki values of 8.97 and 99.70 μM, for ASADH and HL4-DR4 complex, respectively, suggesting potent inhibitory activity. The docking results are visually depicted in Fig. 4 and Fig. S5, illustrating the interactions

between the moringin and ASADH and HLA-DR4 complex, respectively. Moringin formed several hydrogen bonds with the active sites, including Ala12, Ala50, Asp25 in ASADH and Thr130, Thr129 in the HLA-DR4 complex.

4. Discussion

The efficacy of plant-based antibiofilm extracts, fractions or compounds have been extensively studied, however, research focused on their effectiveness against mucoid and SCV biofilms formed by *P. aeruginosa* and *S. aureus* remains limited. Therefore, this study aimed to address this gap by evaluating the potential of 21 plant extracts of seven different biomasses to inhibit bacterial biofilm formation, chemically characterizing their composition, identifying promising extracts, and gaining insights into their mechanism of action. This work paves the way for further studies on developing drugs to combat biofilms present in CF lungs.

The results indicated substantial variability in antioxidant activity across different extracts varying with the solvent and the biomass used. Extractions with ethanol 96 % generally yielded lower antioxidant activities because phenolic compounds, which are well-known for their potential for scavenging free radicals, are typically better extracted with hydroethanolic solvents with intermediate ethanol concentration (50–80 %) [51]. The antioxidant activity of the phenolic compounds is due to the availability of their phenolic hydroxyl groups that can donate their electron or hydrogen, thereby forming stable end products [52,53]. In this study, a higher extraction yield of phenolic compounds did not constantly correspond to a higher content of phenolic compounds in the extract, suggesting that other compounds were also co-extracted.

Given different solvents produced extracts with distinct chemical compositions, it is not surprising that varying levels of biofilm inhibition were observed. Our screening first systematically compared the antibiofilm activity of ethanolic versus aqueous extracts. In general, ethanolic extracts are described as excellent antibiofilm agents, in opposite to the weak activity of aqueous extracts [51,54]. For instance, Alam et al. (2020) reported superior antibiofilm activity of ethanolic and methanolic extracts of *Bergenia ciliata* compared to the aqueous extract that showed the lowest activity [55]. The increased activity of ethanolic
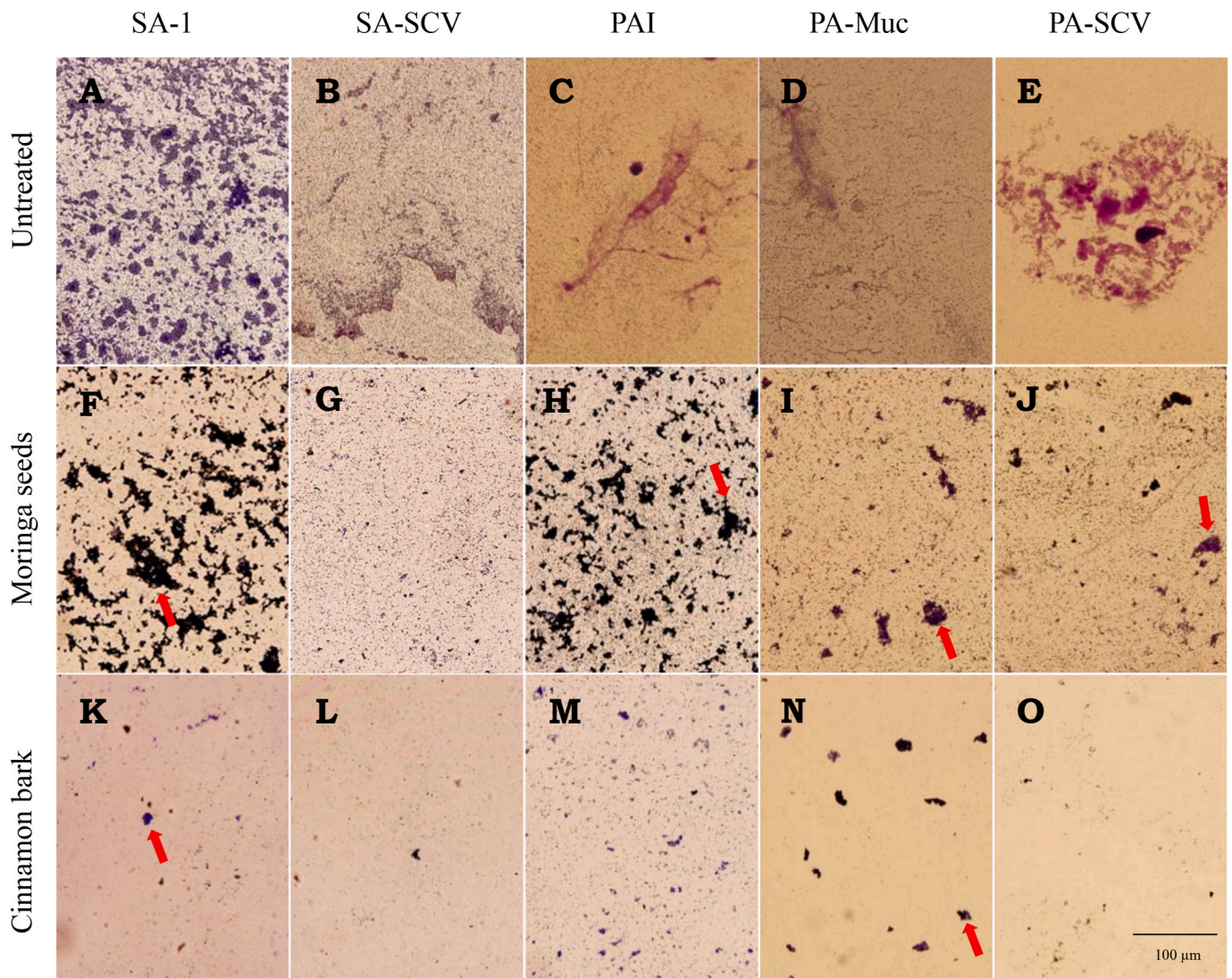
	SA-1	SA-SCV	PAI	PA-Muc	PA-SCV
Untreated	A	B	C	D	E
Moringa seeds	F	G	H	I	J
Cinnamon bark	K	L	M	N	O

100 μm

Fig. 3. Micrographs of bacterial biofilms formed by *P. aeruginosa* (PAI, PA-Muc and PA-SCV) and *S. aureus* strains (SA-1 and SA-SCV) on a plastic coverslip visualized by brightfield microscopy (at 10× magnification). **(A, B, C, D, E)** Untreated control, **(F, G, H, I, J)** treated with 3.3 mg/mL of moringa seeds aqueous extract and **(K, L, M, N, O)** treated with 1.6 mg/mL of cinnamon bark aqueous extract. Red arrows indicate some of the residues left by the extracts. (For interpretation of the references to colour in this figure legend, the reader is referred to the Web version of this article.)

Table 3
Potential *P. aeruginosa* and *S. aureus*-related targets of moringin predicted by PharmMapper.

PDB ID	Protein name	Organism	No. of pharmacophore	Fit-score
2HJS	aspartate-semialdehyde dehydrogenase	*Pseudomonas aeruginosa* PAO1	5	2.949
1D5M	HLA-DR4 complexed with peptide and SEB[a]	*Staphylococcus aureus*	5	2.847

[a] *Staphylococcus aureus* enterotoxin B.

Table 4
Binding energy and interacting active site residues of target proteins with moringin.

Ligand	Binding energy (kcal mol^{-1})	Inhibition constant (Ki, μM)	Active site aminoacids	Interaction type
aspartate-semialdehyde dehydrogenase	−6.89	8.97	A/ALA.12, A/ALA.50, A/ASP.25 A/GLY.48, A/PHE.49 A/GLU.18 A/VAL.21	Hydrogen bond Carbon hydrogen bond Pi-anion Pi-Alkyl
HLA-DR4 complexed with peptide and SEB[a]	−5.46	99.70	A/THR.130, A/THR.129 A/ARG.123, A/PRO.127 A/VAL.128	Hydrogen bond Carbon hydrogen bond Pi-Alkyl

[a] *Staphylococcus aureus* enterotoxin B.

extracts is often associated with the higher solubility of phenolic compounds in hydroethanolic mixtures, as previously mentioned [56–58]. However, our findings did not support this general reported trend. For the assayed plants, aqueous extracts outperformed ethanolic extracts in antibiofilm activity. Water-based extracts are particularly attractive for clinical applications due to the lower toxicity of water compared to organic solvents. Similar to our findings, several studies have been
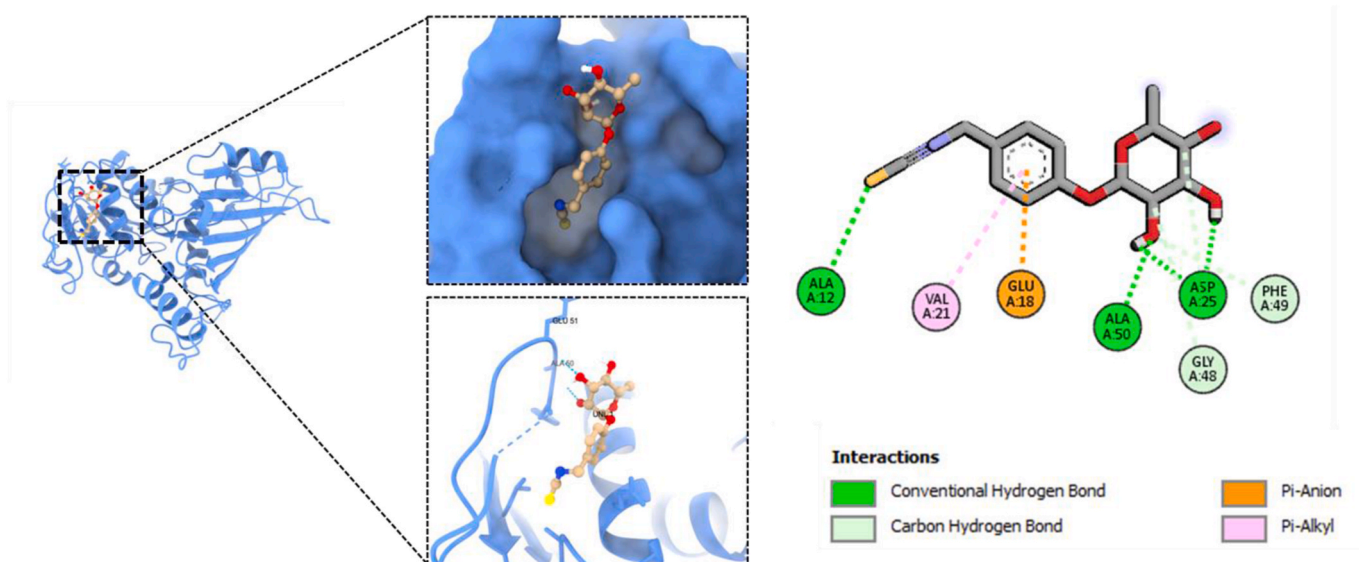
Fig. 4. Molecular interaction between moringin and aspartate-semialdehyde dehydrogenase type of bonds between the proteins and moringin captured by USCF Chimera and Biovia Discovery Studio.

previously reported higher antibiofilm activity for aqueous extracts [27, 59]. For instance, the aqueous extract of the *Cochlospermum regium* flowers showed higher antibiofilm activity against *S. aureus* than the ethanolic extract [59]. The high extraction yield of water can be attributed to the solvent capability to dissolve polar molecules, such as anthocyanins, tannins, saponins, lectins and polypeptides, which may contribute to the extract's superior antibiofilm activity [60,61].

Among the aqueous extracts tested, moringa seed and cinnamon extracts exhibited notable antibiofilm activity against *P. aeruginosa* and *S. aureus*. This is particularly significant in CF, as these two species are frequently co-isolated and their interactions can exacerbate infections by increasing biofilm pathogenesis and persistence [41,62]. The ability of these extracts to inhibit biofilm formation in both species highlights their potential clinical relevance.

Both moringa seeds and cinnamon extracts allowed bacterial adhesion but seemed to discourage the formation of biofilms as no aggregates were observed. This finding led to hypothesize that extracts might act on inhibition of EPS production and/or QS. Similar mechanisms have been reported in other studies, such as downregulation of QS genes and reduction of EPS production in *P. aeruginosa* by *Agrimonia pilosa* Ledeb. [63], and reduction of bacterial attachment to the surface and decreased expression of virulence factors that are regulated by QS, such as pyocyanin, pyoverdine and swimming mobility by *Camelia sinensis* (L.) Kuntze [26].

Moringa is a member of the Moringaceae family and most of its parts including roots, leaves, seeds have been historically used in folk medicine to help cure several diseases. Various studies have confirmed the therapeutic proprieties of moringa, including its antibiofilm activity [64–68]. For instance, an aqueous extract of moringa seeds showed antibiofilm activity against *S. aureus* by destroying the structure of mature biofilms formed in polyvinyl chloride surfaces [69]. Although the moringa extract and the culture medium (milk) used in that study differ from our study, similar activity with the aqueous extract of moringa seeds against mucoid and SCV *P. aeruginosa* and *S. aureus* was found.

Given the promising antibiofilm potential of moringa extract, some studies have isolated and tested compounds from moringa seeds. For instance, Onsare et al. (2015) reported the antibiofilm activity of flavonoids isolated from the seed coat of moringa against *S. aureus*, *P. aeruginosa* and *Candida albicans* [70]. Likewise, a lectin isolated from these seeds inhibited biofilm formation in other Gram-negative bacteria

such as *Serratia marcescens* and *Bacillus* spp [71]. In our study, HPLC-TOF-MS identified benzaldehyde and moringin as the most abundant compounds in the moringa seed extract. The presence of these compounds aligns with previous reports [72,73]. Benzaldehyde, an aromatic aldehyde with a benzene ring, has shown both antimicrobial and antibiofilm activity against *S. aureus*, *E. coli* and *P. aeruginosa* [74]. Leitão et al. (2024) demonstrated that benzaldehyde blocked QS in *P. aeruginosa* and increased its susceptibility to ciprofloxacin [75]. Moringin (or [4-(alpha-L-rhamnosyloxy) benzyl isothiocyanate]), an isothiocyanate compound derived from glucosinolates, has also shown antibacterial activity against *S. aureus* [76,77] and *Listeria monocytogenes* [78]. Despite moringin's higher solubility in ethanol, our aqueous extract showed a strong presence of this compound, likely due to co-extraction with other compounds. Further, isothiocyanates (including moringin) are highly reactive compounds that result from the hydrolysis of glucosinolates (e.g., glucomoringin) and can easily bound to other molecules that have nucleophiles such as hydroxyl, amino or thyol groups. Although moringin is more soluble in ethanol in its free form, its extraction from moringa by-products may be possible using water under certain conditions. This may be due to various complexes formed between various compounds present in this biomass, such as polysaccharides and proteins. For instance, Leone et al. reported 18.4 g/100 g dry weight of carbohydrates and 31 g/100 g dry weight of protein [79]. Moringin can easily bound both to polysaccharides and/or to proteins and be extracted as a complex. Additionally, moringin seeds have a high amount of saponins, that usually mat act as natural surfactant and facilitate the extraction of moringin [80]. This may explain the strong antibiofilm activity of the aqueous extract of moringa seeds.

Cinnamon, also known as Chinese cinnamon, is an evergreen tree commonly found in China and one of the oldest spices in the world. In addition to its role as a culinary spice, it has been traditionally used in various cultures as a remedy for colds and gastrointestinal problems [81]. Cinnamon bark has shown antibiofilm activity against Gram-negative bacteria, such as *P. aeruginosa*, *E. coli*, *Acinetobacter baumannii* and periodontal pathogens [82–85]. For instance, cinnamon oil inhibited biofilm formation in *P. aeruginosa*, making the bacterial cells appear scattered on the surface [84]. Similarly, an ethanolic extract reduced EPS and disrupted *E. coli* biofilm structure, only allowing to form scattered microcolonies [85]. However, in our study, antibiofilm activity was associated with the aqueous extract of cinnamon rather than the ethanolic extract, which may be a result of the extraction

process. Several bioactive compounds from cinnamon extracts with described antibiofilm activity were found in our HPLC-TOF-MS analysis. Quinic acid and coumarin were the most abundant compounds, confirming the composition found in the literature [86]. Quinic acid has been shown to reduce biofilm formation in *P. aeruginosa* by down-regulating the QS system [87], while coumarin has been reported as an inhibitor of several virulence factors involved in biofilm formation in *P. aeruginosa* [88,89]. Moringin was also detected in the aqueous extract of cinnamon. Its increased abundance in the most effective antibiofilm extracts, moringa seeds and cinnamon, against both *P. aeruginosa* and *S. aureus* suggest moringin may play a central role in their antibiofilm activity. However, the aqueous extract of moringa leaves, despite having a high concentration of moringin, did not show antibiofilm activity. These distinct activities among extracts with high moringin content might be attributed to moringin interaction with diverse compounds present in each of the extracts. For instance, compounds in lower proportions in the moringa leaf extract might exert an antagonistic effect inhibiting the antibiofilm activity of moringin. Likewise, compounds unique to the extracts of moringa seeds and cinnamon, and absent in moringa leaf extract, might be enhancing moringin activity through synergistic or additive interactions. Additionally, other components not identified in this study, such as proteins or carbohydrates, might also influence the moringin bioavailability [90].

To explore if moringin could be responsible for the antibiofilm activity, we used PharmMapper to identify potential bacterial targets of this compound. PharmMapper is an open web server that employs reverse pharmacophore mapping to identify potential drug targets [42]. It automatically identifies the optimal mapping poses of the query molecule against all pharmacophore models in PharmTargetDB, providing a list of the top N best-fitted hits along with target annotations and the aligned poses of the respective molecules. In this study, PharmMapper identified ASADH and HLA-DR4 complexed with peptide and SEB as the main targets in *P. aeruginosa* and *S. aureus*, respectively.

ASADH is a crucial enzyme involved in the biosynthesis of essential amino acids and metabolites in microorganisms [91,92]. Inhibition of ASADH has been proposed as a potential strategy for developing drugs to combat multidrug-resistant organisms [93–95]. Since humans and other mammals lack a homolog of ASADH and do not rely on the aspartate biosynthetic pathway, ASADH represents a particularly promising target in microorganisms. However, when microorganisms are deprived of essential amino acids, they often activate alternative transport mechanisms to obtain the amino acid from the environment [92], which may explain the *P. aeruginosa* viability after exposure to moringa and cinnamon extracts. The potential of distinct phytochemicals, such as rosmarinic acid and curcumin, to inhibit ASADH has been previously reported [96].

Molecular docking analysis supported moringin binding to ASADH. Notably, proper intermolecular hydrogen bonding interactions were observed, which is crucial for stable binding and effective inhibition. Moreover, the docking results showed a lower inhibition constant, suggesting that moringin exhibits potent inhibitory effects on this target protein.

The identification of HLA-DR4 complexed with peptide and SEB as a potential target of moringin by PharmMapper suggests a possible immunomodulatory activity, which could be particularly relevant in complex diseases such CF. However, as our experiments were conducted *in vitro* without host immune components, it is likely that moringin also interacts with other bacterial targets that remain unidentified. This finding highlights the importance of further investigating moringin's activity against biofilm-associated bacteria to better understand its mechanisms of action and therapeutic potential.

In conclusion, our study demonstrated that aqueous extracts from moringa seeds and cinnamon bark have significant potential as inhibitors of biofilm formation in *S. aureus* and *P. aeruginosa* clinical isolates with diversified phenotypes, including SCV and mucoid phenotype. The strong antibiofilm activity observed may be attributed to

compounds in higher proportions such as coumarin, quinic acid, and moringin in cinnamon, and benzaldehyde and moringin in moringa seeds, based on literature reports. Notably, moringin, a compound highly prevalent in both extracts, might play a central role in the observed antibiofilm activity. Computational analyses suggested that moringin could be a potential inhibitor of aspartate-semialdehyde dehydrogenase in *P. aeruginosa* and potentially interact with an unknown target in *S. aureus*.

Although our findings highlighted that moringin is a promising antibiofilm agent against mucoid and SCV *P. aeruginosa* and *S. aureus*, the current study is limited to computational predictions and *in vitro* screening. Further experimental studies are necessary to validate the identified target in *P. aeruginosa* and identify the specific target in *S. aureus*, elucidate the mechanisms of action, and assess the therapeutic potential of moringin in treating biofilm-associated infections. Additionally, future work should focus on investigating potential synergistic or antagonistic interactions among extract components to better understand the key contributors of plant-based antibiofilm activity.

CRediT authorship contribution statement

Eduarda Silva: Writing – review & editing, Writing – original draft, Investigation, Formal analysis, Data curation. **Pedro Ferreira-Santos:** Writing – review & editing, Data curation. **José A. Teixeira:** Writing – review & editing. **Maria Olivia Pereira:** Writing – review & editing. **Cristina M.R. Rocha:** Writing – review & editing, Validation, Conceptualization. **Ana Margarida Sousa:** Writing – review & editing, Validation, Supervision.

Declaration of interests

The authors declare that they have no known competing financial interests or personal relationships that could have appeared to influence the work reported in this paper.

Funding and Acknowledgements

Appendix A. Supplementary data

Supplementary data to this article can be found online at https://doi.org/10.1016/j.bioflm.2024.100250.

Data availability

Data will be made available on request.

References

[1] Ratjen F, Bell SC, Rowe SM, Goss CH, Quittner AL, Bush A. Cystic fibrosis. Nat Rev Dis Prim 2015;1:15010. https://doi.org/10.1038/nrdp.2015.10.

[2] Bhagirath AY, Li Y, Somayajula D, Dadashi M, Badr S, Duan K. Cystic fibrosis lung environment and Pseudomonas aeruginosa infection. BMC Pulm Med 2016;16:174. https://doi.org/10.1186/s12890-016-0339-5.

[3] Cystic Fibrosis Foundation. Cystic Fibrosis Foundation Patient Registry 2020. Annual data report. Bethesda: Maryland; 2021.

[4] Vetrivel A, Ramasamy M, Vetrivel P, Natchimuthu S, Arunachalam S, Kim G-S, et al. Pseudomonas aeruginosa biofilm formation and its control. Biologics 2021;1:312–36. https://doi.org/10.3390/biologics1030019.

[5] Thi MTT, Wibowo D, Rehm BHA. Pseudomonas aeruginosa biofilms. Int J Mol Sci 2020;21:8671. https://doi.org/10.3390/ijms21228671.

[6] Taylor PK, Yeung ATY, Hancock REW. Antibiotic resistance in Pseudomonas aeruginosa biofilms: towards the development of novel anti-biofilm therapies. J Biotechnol 2014;191:121–30. https://doi.org/10.1016/j.jbiotec.2014.09.003.

[7] Sousa AM, Pereira MO. Pseudomonas aeruginosa diversification during infection development in cystic fibrosis lungs-a review. Pathogens 2014;3:680–703. https://doi.org/10.3390/pathogens3030680.

[8] Beaudoin T, Yau YCW, Stapleton PJ, Gong Y, Wang PW, Guttman DS, et al. Staphylococcus aureus interaction with Pseudomonas aeruginosa biofilm enhances tobramycin resistance. Npj Biofilms Microbiomes 2017;3:25. https://doi.org/10.1038/s41522-017-0035-0.

[9] Monteiro R, Magalhães AP, Pereira MO, Sousa AM. Long-term coexistence of Pseudomonas aeruginosa and Staphylococcus aureus using an in vitro cystic fibrosis model. Future Microbiol 2021;16:879–93. https://doi.org/10.2217/fmb-2021-0025.

[10] Hubert D, Réglier-Poupet H, Sermet-Gaudelus I, Ferroni A, Le Bourgeois M, Burgel P-R, et al. Association between Staphylococcus aureus alone or combined with Pseudomonas aeruginosa and the clinical condition of patients with cystic fibrosis. J Cyst Fibros 2013;12:497–503. https://doi.org/10.1016/j.jcf.2012.12.003.

[11] Kahl BC. Small colony variants (SCVs) of Staphylococcus aureus – a bacterial survival strategy. Infect Genet Evol 2014;21:515–22. https://doi.org/10.1016/j.meegid.2013.05.016.

[12] Malone J. Role of small colony variants in persistence of Pseudomonas aeruginosa infections in cystic fibrosis lungs. Infect Drug Resist 2015;8:237. https://doi.org/10.2147/IDR.S68214.

[13] Evans TJ. Small colony variants of Pseudomonas aeruginosa in chronic bacterial infection of the lung in cystic fibrosis. Future Microbiol 2015;10:231–9. https://doi.org/10.2217/fmb.14.107.

[14] Kahl BC, Becker K, Löffler B. Clinical significance and pathogenesis of staphylococcal small colony variants in persistent infections. Clin Microbiol Rev 2016;29:401–27. https://doi.org/10.1128/CMR.00069-15.

[15] Purevdorj-Gage B, Costerton WJ, Stoodley P. Phenotypic differentiation and seeding dispersal in non-mucoid and mucoid Pseudomonas aeruginosa biofilms. Microbiology 2005;151:1569–76. https://doi.org/10.1099/mic.0.27536-0.

[16] Folkesson A, Jelsbak L, Yang L, Johansen HK, Ciofu O, Høiby N, et al. Adaptation of Pseudomonas aeruginosa to the cystic fibrosis airway: an evolutionary perspective. Nat Rev Microbiol 2012;10:841–51. https://doi.org/10.1038/nrmicro2907.

[17] Høiby N, Bjarnsholt T, Givskov M, Molin S, Ciofu O. Antibiotic resistance of bacterial biofilms. Int J Antimicrob Agents 2010;35:322–32. https://doi.org/10.1016/j.ijantimicag.2009.12.011.

[18] Zolin A, Orenti A, Jung A, van Rens J, Al E. ECFSPR annual report 2021. 2023.

[19] Tewkesbury DH, Robey RC, Barry PJ. Progress in precision medicine in cystic fibrosis: a focus on CFTR modulator therapy. Breathe 2021;17:210112. https://doi.org/10.1183/20734735.0112-2021.

[20] Quon BS, Rowe SM. New and emerging targeted therapies for cystic fibrosis. BMJ 2016;352:i859. https://doi.org/10.1136/bmj.i859.

[21] Foundation CF. Cystic fibrosis foundation patient registry - 2023 annual data report. 2024.

[22] Kalan L, Wright GD. Antibiotic adjuvants: multicomponent anti-infective strategies. Expet Rev Mol Med 2011;13:e5. https://doi.org/10.1017/S1462399410001766.

[23] Mishra R, Panda AK, De Mandal S, Shakeel M, Bisht SS, Khan J. Natural anti-biofilm agents: strategies to control biofilm-forming pathogens. Front Microbiol 2020;11:2640. https://doi.org/10.3389/fmicb.2020.566325.

[24] Álvarez-Martínez FJ, Barrajón-Catalán E, Micol V. Tackling antibiotic resistance with compounds of natural origin: a comprehensive review. Biomedicines 2020;8:405. https://doi.org/10.3390/biomedicines8100405.

[25] Silva E, Teixeira JA, Pereira MO, Rocha CMR, Sousa AM. Evolving biofilm inhibition and eradication in clinical settings through plant-based antibiofilm agents. Phytomedicine 2023;119:154973. https://doi.org/10.1016/j.phymed.2023.154973.

[26] Qais FA, Khan MS, Ahmad I. Broad-spectrum quorum sensing and biofilm inhibition by green tea against gram-negative pathogenic bacteria: deciphering the role of phytocompounds through molecular modelling. Microb Pathog 2019;126:379–92. https://doi.org/10.1016/j.micpath.2018.11.030.

[27] Von Borowski RG, Zimmer KR, Leonardi BF, Trentin DS, Silva RC, de Barros MP, et al. Red pepper Capsicum baccatum: source of antiadhesive and antibiofilm compounds against nosocomial bacteria. Ind Crops Prod 2019;127:148–57. https://doi.org/10.1016/j.indcrop.2018.10.011.

[28] Noumi E, Merghni A, M Alreshidi M, Haddad O, Akmadar G, De Martino L, et al. Chromobacterium violaceum and Pseudomonas aeruginosa PAO1: models for evaluating anti-quorum sensing activity of Melaleuca alternifolia essential oil and its main component terpinen-4-ol. Molecules 2018;23:2672. https://doi.org/10.3390/molecules23102672.

[29] Santiago C, Lim K-H, Loh H-S, Ting K. Inhibitory effect of Duabanga grandiflora on MRSA biofilm formation via prevention of cell-surface attachment and PBP2a production. Molecules 2015;20:4473–82. https://doi.org/10.3390/molecules20034473.

[30] Choi N-Y, Kang S-Y, Kim K-J. Artemisia princeps inhibits biofilm formation and virulence-factor expression of antibiotic-resistant bacteria. BioMed Res Int 2015;2015:1–7. https://doi.org/10.1155/2015/239519.

[31] Lee J-H, Kim Y-G, Ryu SY, Cho MH, Lee J. Ginkgolic acids and Ginkgo biloba extract inhibit Escherichia coli O157:H7 and Staphylococcus aureus biofilm

formation. Int J Food Microbiol 2014;174:47–55. https://doi.org/10.1016/j.ijfoodmicro.2013.12.030.

[32] Zhang J, Rui X, Wang L, Guan Y, Sun X, Dong M. Polyphenolic extract from Rosa rugosa tea inhibits bacterial quorum sensing and biofilm formation. Food Control 2014;42:125–31. https://doi.org/10.1016/j.foodcont.2014.02.001.

[33] Rajasekharan SK, Ramesh S, Satish AS, Lee J. Antibiofilm and anti-β-lactamase activities of burdock root extract and chlorogenic acid against Klebsiella pneumoniae. J Microbiol Biotechnol 2017;27:542–51. https://doi.org/10.4014/jmb.1609.09043.

[34] Abreu AC, Coqueiro A, Sultan AR, Lemmens N, Kim HK, Verpoorte R, et al. Looking to nature for a new concept in antimicrobial treatments: isoflavonoids from Cytisus striatus as antibiotic adjuvants against MRSA. Sci Rep 2017;7:3777. https://doi.org/10.1038/s41598-017-03716-7.

[35] da Silva Gündel S, de Souza ME, Quatrin PM, Klein B, Wagner R, Gündel A, et al. Nanoemulsions containing Cymbopogon flexuosus essential oil: development, characterization, stability study and evaluation of antimicrobial and antibiofilm activities. Microb Pathog 2018;118:268–76. https://doi.org/10.1016/j.micpath.2018.03.043.

[36] Ferreira-Santos P, Genisheva Z, Botelho C, Santos J, Ramos C, Teixeira JA, et al. Unravelling the biological potential of Pinus pinaster bark extracts. Antioxidants 2020;9:334. https://doi.org/10.3390/antiox9040334.

[37] Meneses NGT, Martins S, Teixeira JA, Mussatto SI. Influence of extraction solvents on the recovery of antioxidant phenolic compounds from brewer's spent grains. Sep Purif Technol 2013;108:152–8. https://doi.org/10.1016/j.seppur.2013.02.015.

[38] Ballesteros LF, Cerqueira MA, Teixeira JA, Mussatto SI. Characterization of polysaccharides extracted from spent coffee grounds by alkali pretreatment. Carbohydr Polym 2015;127:347–54. https://doi.org/10.1016/j.carbpol.2015.03.047.

[39] Singleton VL, Orthofer R, Lamuela-Raventós RM. [14] Analysis of total phenols and other oxidation substrates and antioxidants by means of folin-ciocalteu reagent. Methods Enzymol 1999;152:78. https://doi.org/10.1016/S0076-6879(99)99017-1.

[40] Peeters E, Nelis HJ, Coenye T. Comparison of multiple methods for quantification of microbial biofilms grown in microtiter plates. J Microbiol Methods 2008;72:157–65. https://doi.org/10.1016/j.mimet.2007.11.010.

[41] Magalhães AP, Lopes SP, Pereira MO. Insights into cystic fibrosis polymicrobial consortia: the role of species interactions in biofilm development, phenotype, and response to in-use anatibiotics. Front Microbiol 2017;7. https://doi.org/10.3389/fmicb.2016.02146.

[42] PharmMapper n.d. http://www.lilab-ecust.cn/pharmmapper/. [Accessed 1 April 2024].

[43] Wang X, Shen Y, Wang S, Li S, Zhang W, Liu X, et al. PharmMapper 2017 update: a web server for potential drug target identification with a comprehensive target pharmacophore database. Nucleic Acids Res 2017;45:W356–60. https://doi.org/10.1093/nar/gkx374.

[44] Liu X, Ouyang S, Yu B, Liu Y, Huang K, Gong J, et al. PharmMapper server: a web server for potential drug target identification using pharmacophore mapping approach. Nucleic Acids Res 2010;38:W609–14. https://doi.org/10.1093/nar/gkq300.

[45] Rcsb PDB: Homepage n.d. https://www.rcsb.org/. [Accessed April 2024].

[46] PubChem n.d. https://pubchem.ncbi.nlm.nih.gov/. [Accessed 1 April 2024].

[47] Morris GM, Ruth H, Lindstrom W, Sanner MF, Belew RK, Goodsell DS, et al. Software news and updates AutoDock4 and AutoDockTools4: automated docking with selective receptor flexibility. J Comput Chem 2009;30:2785–91. https://doi.org/10.1002/jcc.21256.

[48] Pettersen EF, Goddard TD, Huang CC, Couch GS, Greenblatt DM, Meng EC, et al. UCSF Chimera - a visualization system for exploratory research and analysis. J Comput Chem 2004;25:1605–12. https://doi.org/10.1002/jcc.20084.

[49] Kim J, Urban RG, Strominger JL, Wiley DC. Toxic shock syndrome toxin-1 complexed with a class II major histocompatibility molecule HLA-DR1. Science (80-) 1994;266:1870–4. https://doi.org/10.1126/science.7997880.

[50] Komisar JL, Small-Harris S, Tseng J. Localization of binding sites of staphylococcal enterotoxin B (SEB), a superantigen, for HLA-DR by inhibition with synthetic peptides of SEB. Infect Immun 1994;62:4775–80. https://doi.org/10.1128/iai.62.11.4775-4780.1994.

[51] Muflihah YM, Gollavelli G, Ling YC. Correlation study of antioxidant activity with phenolic and flavonoid compounds in 12 Indonesian indigenous herbs. Antioxidants 2021;10. https://doi.org/10.3390/antiox10101530.

[52] Soobrattee MA, Neergheen VS, Luximon-Ramma A, Aruoma OI, Bahorun T. Phenolics as potential antioxidant therapeutic agents: mechanism and actions. Mutat Res, Fundam Mol Mech Mutagen 2005;579:200–13. https://doi.org/10.1016/j.mrfmmm.2005.03.023.

[53] Elzaawely AA, Xuan TD, Koyama H, Tawata S. Antioxidant activity and contents of essential oil and phenolic compounds in flowers and seeds of Alpinia zerumbet (Pers.) B.L. Burtt. & R.M. Sm. Food Chem 2007;104:1648–53. https://doi.org/10.1016/j.foodchem.2007.03.016.

[54] Idir F, Van Ginneken S, Coppola GA, Grenier D, Steenackers HP, Bendali F. Origanum vulgare ethanolic extracts as a promising source of compounds with antimicrobial, anti-biofilm, and anti-virulence activity against dental plaque bacteria. Front Microbiol 2022;13:4256. https://doi.org/10.3389/fmicb.2022.999839.

[55] Alam K, Farraj DA Al, Mah-e-Fatima S, Yameen MA, Elshikh MS, Alkufeidy RM, et al. Anti-biofilm activity of plant derived extracts against infectious pathogen-Pseudomonas aeruginosa PAO1. J Infect Public Health 2020;13:1734–41. https://doi.org/10.1016/j.jiph.2020.07.007.

[56] Anwar F., Przybylski R. Effect of solvents extraction on total phenolics and antioxidant activity of extracts from flaxseed (Linum usitatissimum L.). Acta Sci Pol Technol Aliment 2012;11:293–301. PMID: 22744950.

[57] Kaczorová D, Karalija E, Dahija S, Bešta-Gajević R, Parić A, Ćavar Zeljković S. Influence of extraction solvent on the phenolic profile and bioactivity of two Achillea species. Molecules 2021;26:1601. https://doi.org/10.3390/molecules26061601.

[58] Oliveira DM, Melo FG, Balogun SO, Flach A, de Souza ECA, de Souza GP, et al. Antibacterial mode of action of the hydroethanolic extract of Leonotis nepetifolia (L.) R. Br. involves bacterial membrane perturbations. J Ethnopharmacol 2015;172:356–63. https://doi.org/10.1016/j.jep.2015.06.027.

[59] Galvão F de O, Dantas FG da S, Santos CR, de L, Marchioro SB, Cardoso CAL, Wender H, et al. Cochlospermum regium (Schrank) pilger leaf extract inhibit methicillin-resistant Staphylococcus aureus biofilm formation. J Ethnopharmacol 2020;261:113167. https://doi.org/10.1016/j.jep.2020.113167.

[60] Cowan MM. Plant products as antimicrobial agents. Clin Microbiol Rev 1999;12:564–82. https://doi.org/10.1128/CMR.12.4.564.

[61] Nortjie E, Basitere M, Moyo D, Nyamukamba P. Extraction methods, quantitative and qualitative phytochemical screening of medicinal plants for antimicrobial textiles: a review. Plants 2022;11:2011. https://doi.org/10.3390/plants11152011.

[62] Reece E, Bettio PH de A, Renwick J. Polymicrobial interactions in the cystic fibrosis airway microbiome impact the antimicrobial susceptibility of Pseudomonas aeruginosa. Antibiotics 2021;10:827. https://doi.org/10.3390/antibiotics10070827.

[63] Wang S, Feng Y, Han X, Cai X, Yang L, Liu C, et al. Inhibition of virulence factors and biofilm formation by wogonin attenuates pathogenicity of Pseudomonas aeruginosa PAO1 via targeting pqs quorum-sensing system. Int J Mol Sci 2021;22:12699. https://doi.org/10.3390/ijms222312699.

[64] Pareek A, Pant M, Gupta MM, Kashania P, Ratan Y, Jain V, et al. Moringa oleifera: an updated comprehensive review of its pharmacological activities, ethnomedicinal, phytopharmaceutical formulation, clinical, phytochemical, and toxicological aspects. Int J Mol Sci 2023;24:2098. https://doi.org/10.3390/ijms24032098.

[65] Saini RK, Sivanesan I, Keum Y-S. Phytochemicals of Moringa oleifera: a review of their nutritional, therapeutic and industrial significance. 3 Biotech 2016;6:203. https://doi.org/10.1007/s13205-016-0526-3.

[66] Muhammad AA, Pauzi NAS, Arulselvan P, Abas F, Fakurazi S. In vitro wound healing potential and identification of bioactive compounds from Moringa oleifera Lam. BioMed Res Int 2013;2013:1–10. https://doi.org/10.1155/2013/974580.

[67] Amin MF, Ariwibowo T, Putri SA, Kurnia D. Moringa oleifera: a review of the pharmacology, chemical constituents, and application for dental health. Pharmaceuticals 2024;17. https://doi.org/10.3390/ph17010142.

[68] Dayal B, Yannamreddy VR, Ragunath C, Ramasubbu N, Roy T, Amin R, et al. Breaking up of biofilms with Moringa oleifera: insights into mechanisms. ACS Symp. Ser., vol. 1143, American Chemical Society 2013:177–91. https://doi.org/10.1021/bk-2013-1143.ch010.

[69] De Oliveira AM, Da Silva Férnandes M, De Abreu Filho BA, Gomes RG, Bergamasco R. Inhibition and removal of staphylococcal biofilms using Moringa oleifera Lam. aqueous and saline extracts. J Environ Chem Eng 2018;6:2011–6. https://doi.org/10.1016/j.jece.2018.02.043.

[70] Onsare JG, Arora DS. Antibiofilm potential of flavonoids extracted from Moringa oleifera seed coat against Staphylococcus aureus , Pseudomonas aeruginosa and Candida albicans. J Appl Microbiol 2015;118:313–25. https://doi.org/10.1111/jam.12701.

[71] Moura MC, Trentin DS, Napoleão TH, Primon-Barros M, Xavier AS, Carneiro NP, et al. Multi-effect of the water-soluble Moringa oleifera lectin against Serratia marcescens and Bacillus sp.: antibacterial, antibiofilm and anti-adhesive properties. J Appl Microbiol 2017;123:861–74. https://doi.org/10.1111/jam.13556.

[72] Tang M-M, Chen G-Y, Jiang K-C, Luo M-Y, Wu H, Hu B, et al. A new phenolic glycoside from the seeds of Moringa oleifera. Chem Nat Compd 2020;56:642–4. https://doi.org/10.1007/s10600-020-03112-0.

[73] Mathiron D, Iori R, Pilard S, Soundara Rajan T, Landy D, Mazzon E, et al. A combined approach of NMR and mass spectrometry techniques applied to the α-cyclodextrin/moringin complex for a novel bioactive formulation. Molecules 2018;23:1714. https://doi.org/10.3390/molecules23071714.

[74] Fathallah N, Raafat MM, Issa MY, Abdel-Aziz MM, Bishr M, Abdelkawy MA, et al. Bio-guided fractionation of prenylated benzaldehyde derivatives as potent antimicrobial and antibiofilm from Ammi majus L. fruits-associated Aspergillus amstelodami. Molecules 2019;24:4118. https://doi.org/10.3390/molecules24224118.

[75] Leitão MM, Vieira TF, Sousa SF, Borges F, Simões M, Borges A. Dual action of benzaldehydes: inhibiting quorum sensing and enhancing antibiotic efficacy for controlling Pseudomonas aeruginosa biofilms. Microb Pathog 2024;191:106663. https://doi.org/10.1016/j.micpath.2024.106663.

[76] Galuppo M, De Nicola GR, Iori R, Dell'Utri P, Bramanti P, Mazzon E. Antibacterial activity of glucomoringin bioactivated with myrosinase against two important

[77] Padla EP, Solis LT, Levida RM, Ragasa CY, Shen CC. Antimicrobial isothiocyanates from the seeds of Moringa oleifera Lam. Zeitschrift Fur Naturforsch 2012;67:557–64. https://doi.org/10.1515/znc-2012-11-1205.

[78] Wen Y, Li W, Su R, Yang M, Zhang N, Li X, et al. Multi-target antibacterial mechanism of moringin from Moringa oleifera seeds against Listeria monocytogenes. Front Microbiol 2022;13:925291. https://doi.org/10.3389/fmicb.2022.925291.

[79] Leone A, Spada A, Battezzati A, Schiraldi A, Aristil J, Bertoli S. Moringa oleifera seeds and oil: characteristics and uses for human health. Int J Mol Sci 2016;17:2141. https://doi.org/10.3390/ijms17122141.

[80] Gu X, Yang Y, Wang Z. Nutritional, phytochemical, antioxidant, α-glucosidase and α-amylase inhibitory properties of Moringa oleifera seeds. South African J Bot 2020;133:151–60. https://doi.org/10.1016/j.sajb.2020.07.021.

[81] Hong J-W, Yang G-E, Kim YB, Eom SH, Lew J-H, Kang H. Anti-inflammatory activity of cinnamon water extract in vivo and in vitro LPS-induced models. BMC Complement Altern Med 2012;12:237. https://doi.org/10.1186/1472-6882-12-237.

[82] Panjaitan CC, Widyarman AS, Amtha R, Astoeti TE. Antimicrobial and antibiofilm activity of cinnamon (Cinnamomum burmanii) extract on periodontal pathogens—an in vitro study. Eur J Dent 2022;16:938–46. https://doi.org/10.1055/s-0041-1742125.

[83] Ganić T, Vuletić S, Nikolić B, Stevanović M, Kuzmanović M, Kekić D, et al. Cinnamon essential oil and its emulsion as efficient antibiofilm agents to combat Acinetobacter baumannii. Front Microbiol 2022;13:989667. https://doi.org/10.3389/fmicb.2022.989667.

[84] Kalia M, Yadav VK, Singh PK, Sharma D, Pandey H, Narvi SS, et al. Effect of cinnamon oil on quorum sensing-controlled virulence factors and biofilm formation in Pseudomonas aeruginosa. PLoS One 2015;10:e0135495. https://doi.org/10.1371/journal.pone.0135495.

[85] Lu C, Liu H, Shangguan W, Chen S, Zhong Q. Antibiofilm activities of the cinnamon extract against Vibrio parahaemolyticus and Escherichia coli. Arch Microbiol 2021;203:125–35. https://doi.org/10.1007/s00203-020-02008-5.

[86] Tang PL, Chen YT, Qin H, Hou X, Deng J. Effect of cinnamon bark and twig extracts on the chemical, physicochemical and antioxidant properties of fermented milk. J Food Meas Charact 2020;14:2271–81. https://doi.org/10.1007/s11694-020-00474-5.

[87] Lu L, Zhao Y, Yi G, Li M, Liao L, Yang C, et al. Quinic acid: a potential antibiofilm agent against clinical resistant Pseudomonas aeruginosa. Chin Med 2021;16:72. https://doi.org/10.1186/s13020-021-00481-8.

[88] Zhang Y, Sass A, Van Acker H, Wille J, Verhasselt B, Van Nieuwerburgh F, et al. Coumarin reduces virulence and biofilm formation in Pseudomonas aeruginosa by affecting quorum sensing, type III secretion and C-di-GMP levels. Front Microbiol 2018;9. https://doi.org/10.3389/fmicb.2018.01952.

[89] Qais FA, Khan MS, Ahmad I, Husain FM, Khan RA, Hassan I, et al. Coumarin exhibits broad-spectrum antibiofilm and antiquorum sensing activity against gram-negative bacteria: in vitro and in silico investigation. ACS Omega 2021;6:18823–35. https://doi.org/10.1021/acsomega.1c02046.

[90] Saucedo-Pompa S, Torres-Castillo JA, Castro-López C, Rojas R, Sánchez-Alejo EJ, Ngangyo-Heya M, et al. Moringa plants: bioactive compounds and promising applications in food products. Food Res Int 2018;111:438–50. https://doi.org/10.1016/J.FOODRES.2018.05.062.

[91] Teakel SL, Fairman JW, Muruthi MM, Abendroth J, Dranow DM, Lorimer DD, et al. Structural characterization of aspartate-semialdehyde dehydrogenase from Pseudomonas aeruginosa and Neisseria gonorrhoeae. Sci Rep 2022;12:14010. https://doi.org/10.1038/s41598-022-17384-9.

[92] Kumar RRR, Diwakar V, Khan N, Kumar Meghwanshi G, Garg P. Structural–functional analysis of drug target aspartate semialdehyde dehydrogenase. Drug Discov Today 2024;29:103908. https://doi.org/10.1016/j.drudis.2024.103908.

[93] Vyas R, Tewari R, Weiss MS, Karthikeyan S. Structures of ternary complexes of aspartate-semialdehyde dehydrogenase (Rv3708c) from Mycobacterium tuberculosis H37Rv. Acta Crystallogr Sect D Biol Crystallogr 2012;68:671–9. https://doi.org/10.1107/S0907444912007330.

[94] Garg A, Tewari R, Raghava GP. Virtual screening of potential drug-like inhibitors against Lysine/DAP pathway of Mycobacterium tuberculosis. BMC Bioinf 2010;11:S53. https://doi.org/10.1186/1471-2105-11-S1-S53.

[95] Luniwal A, Wang L, Pavlovsky A, Erhardt PW, Viola RE. Molecular docking and enzymatic evaluation to identify selective inhibitors of aspartate semialdehyde dehydrogenase. Bioorganic Med Chem 2012;20:2950–6. https://doi.org/10.1016/j.bmc.2012.03.013.

[96] Khan S, Somvanshi P, Bhardwaj T, Mandal RK, Dar SA, Wahid M, et al. Aspartate-β-semialdeyhde dehydrogenase as a potential therapeutic target of Mycobacterium tuberculosis H37Rv: evidence from in silico elementary mode analysis of biological network model. J Cell Biochem 2018;119:2832–42. https://doi.org/10.1002/jcb.26458.